FEDSM 2000-11241

ON THE ONSET AND DEVELOPMENT OF ROTATING STALL WITHIN A VANED DIFFUSER OF A CENTRIFUGAL PUMP

Manish SINHA, Ali PINARBASI and Joseph KATZ
Department of Mechanical Engineering
The Johns Hopkins University
Baltimore, 21218, MD

ABSTRACT

PIV and pressure fluctuation measurements at several sites are used to investigate the onset and development of a rotating stall within a centrifugal pump with vaned diffuser. The experiments are performed in a facility that enables flow visualization in the impeller between the diffuser vanes and in the volute. As the flow rate is reduced from no stall conditions, intermittent separation and reverse flow occur with increasing frequency and magnitude of reverse velocity. The stall cell also increases in size and eventually covers more than two vane passages simultaneously. Reverse flow also occurs within the impeller. Associated with operation well below design conditions, there is a strong "leakage flow" in the gap between the impeller and the diffuser, from the exit side of the tongue to the beginning side with magnitude of about 50% of the impeller tip speed. This leakage flow causes separation on the concave side (suction side in pump terminology) of the diffuser vanes. With decreasing flow rate, this separation initiates the stall process. The paper provides detailed instantaneous and phase averaged velocity distributions at different flow rates both in unstalled and stalled conditions. Phase averaged data is obtained using pressure transducers located with the vane passage. It is shown that the blade orientation has little impact at the flow structure during stall.

INTRODUCTION

At reduced flow rates, the performance, flow rate and pressure, of a compressor or a pump become increasingly unstable. Rotating stall is one such class of unsteady phenomena wherein the flow fluctuations are propagating at a low frequency, but are limited to parts of components (e.g. rotor, diffuser or volute). Numerous studies with different turbomachinery components have already focused a rotating stall. Empirical correlations for the behavior of impellers and diffuser have also been developed (Yoshida et al., 1991; Ogata et al., 1995; Braembussche, 1996; Tsujimoto, 1996; Miyake and Nagata, 1999; Tsurusaki and Kiroshita, 1999). Some computational work, has also been performed, for example by Shuliang et al. (1999) and Longatte and Kueny, (1999). In spite of these efforts, there is still very little experimental data on the detailed flow structures with a stalled turbomachine. The objective of this study is to look at the flow structure in great detail, at different flow rates, both in unstalled and stalled condition. This paper continues a presentation by Sinha and Katz (1999). It is reported there that a high speed jet and a reverse flow alternate in a stalled vane passage. They also indicate close relationship between the onset of stall, its propagation and the non-uniform pressure distribution in the volute.

EXPERIMENTAL PROCEDURE

A schematic of the centrifugal pump rig used in the present study is shown in Figure 1. The pump is vibration isolated and separated from the rest of the facility using 50 m of coiled flexible hoses. Table 1 presents the specification of the facility.

The impeller has backswept blades with a logarithmic profile and the vaned diffuser has straight walls with a constant cross sectional area. Parts of the original stainless steel blades and outer shroud were removed and replaced with acrylic to

allow visual access in the flow within the impeller. The diffuser and outer perimeter of the volute are also transparent.

Table 1. Geometric data and operating conditions

Impeller:

Inlet diameter	8.51 cm
Discharge diameter	20.32 cm
Number of blades	5backswept
Exit angle of blade	21.3°

Operating conditions:

Rotor speed	890 rpm
Design flow rate	5.67 l/s
Design Flow coefficient	0.118
Design specific speed	0.49
Flowrate of the present experiments	2.52 l/s – 3.78 l/s
Flow coefficient of the present experiments	0.052-0.078

Diffuser:

Number of vanes	9
Inside diameter	24.45 cm
Discharge diameter	30.5 cm
Inlet angle of vane	10.6°
Outlet angle of vane	10.97°
Chord length	13.44 cm
Suction side radius	14.15 cm
Pressure side radius	24.79 cm
Axial width	1.27 cm

The setup allows illumination and flow visualization in both the horizontal (parallel to the shrouds) and vertical planes. The configuration of the perimeter of the volute in cm is given by:

$$r_v = 17.78 + 24.46 \text{X } \theta/360 \text{ (}\theta \text{ is between } 0°\text{-}360°\text{)}.$$

In the present configuration the tip of the tongue is located at $\theta=29°$. Beyond $\theta=360°$ the outer perimeter is straight. The 24.46 x 1.27 cm² exit is gradually expanded to a 10.16 cm pipe by imposing a maximum expansion angle of less than 7° to avoid separation. The pump is instrumented with flush mounted piezoelectric pressure transducers, model PCB 105B02, that are mounted on the hub surface, along the center streamline, in six adjacent vane passages. They are labeled A to F in Figure 1.

PIV System

All the data included in the present paper, focuses on the flow near the exit of the pump, as shown in Figure 1. The optical setup of the PIV system is illustrated in Figure 2. A 350 mJ/pulse, Nd:Yag laser and sheet forming optics are similar to the setup used in previous experiments (Sinha et al., 2000a, b).
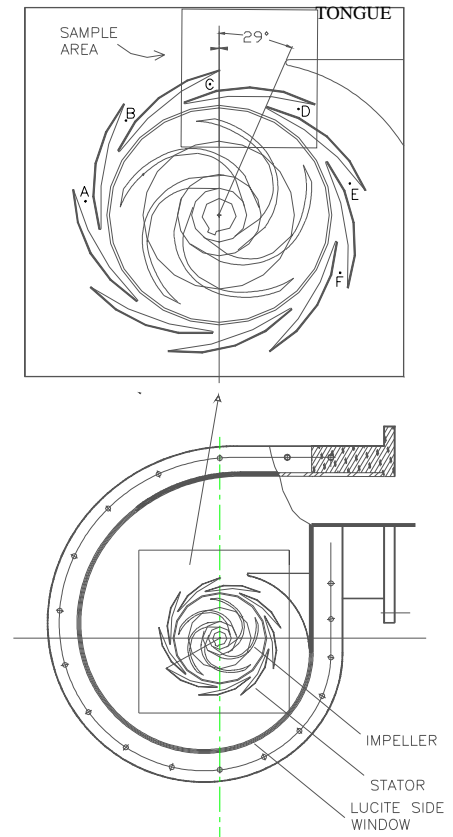

Figure 1. The pump geometry and location of the present measurements.
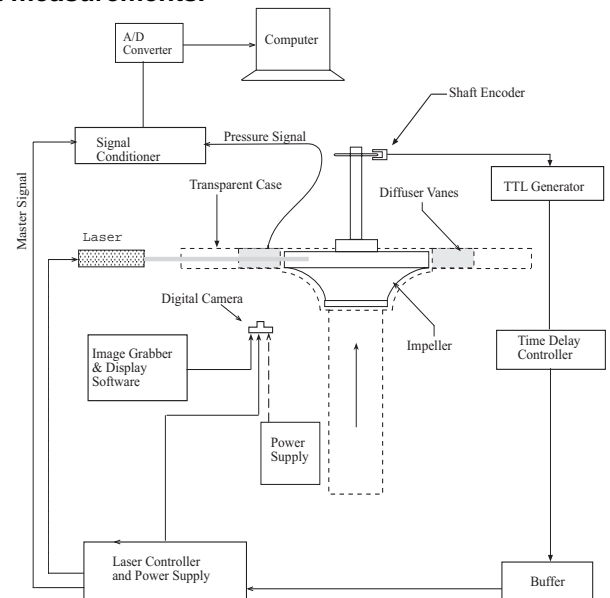

Figure 2. The optical and control system

The images are recorded by a 2048x2048 pixels², 4 frames/s digital camera that incorporate fast digital image shifting (Sinha et. al. 1998) to overcome directional ambiguity. These images are recorded in a controlled fashion at the desired impeller and pressure phase of the transducer located at C. The electronic control unit detects the maximum, minimum and zero-crossing phases of a low-path-filtered pressure signal associated with the stall. A shaft encoder provides information on the impeller blade orientation.
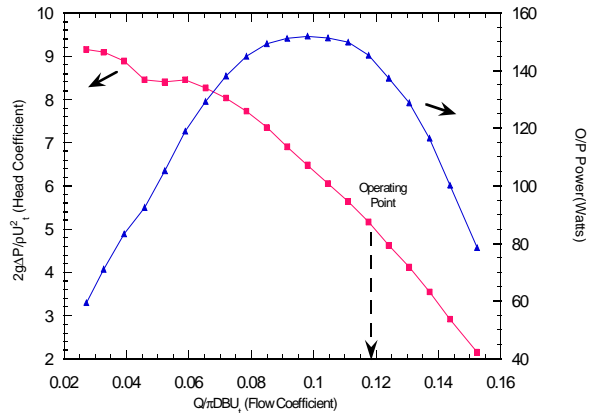
Figure 3. Performance curve of the pump
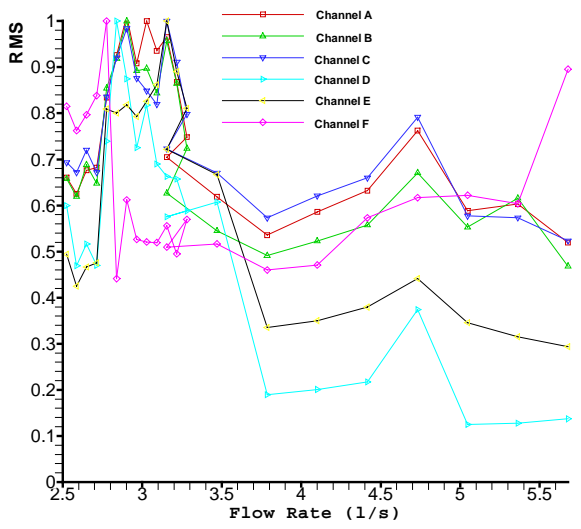
Figure 4. RMS of fluctuations of the dynamic pressure at varying flow rates

The acquired images are enhanced using an in-house histogram equalization algorithm (Bertuccioli et al., 1996; Roth et al, 1995, 1999) and analyzed with in-house auto-correlation software. The window size is 64 x 64 pixel² and the vectors are calculated every 32 pixels, i.e. 50% overlap between neighboring windows. The water is seeded with 20 μm, neutrally buoyant fluorescent particles. The particle concentration is maintained at a level that insures a distribution 7-8 pairs per window. Past calibrations (Roth et al., 1995,1999) have shown that the characteristic uncertainty is about 0.3 pixels – i.e. 0.04 m/s at the present magnification.

RESULTS

A performance curve of the present pump is presented in Figure 3. RMS values of pressure fluctuation in passages A-F, are recorded at different flow rates, starting from 5.67 l/s and lower (Figure 4). Pressure spectra and calculation of stall propagation phase angles have already been presented in Sinha et al. (1999). The stall frequency is about 0.93 Hz, much slower than the 15 Hz shaft frequency and 75 Hz blade-rate frequency. Interestingly, the rms value starts increasing at around 3.78 l/s, for channels A, B, C, and E. The pressure at D, however, starts to rise at about 3.15 l/s and peaks at about 2.84 l/s. Passage F peaks at a much lower flow rate of about 2.52 l/s. Thus, at 3 l/s, passages A, B, C, D, E are already stalled whereas passage F is not. This statement is supported by the calculated stall propagation rates obtained using cross-correlation of pressure signals (Sinha et al.).

As will be demonstrated in this paper, the increased level of fluctuation is caused by massive flow oscillations, from being stalled (reverse flow) to having a jet flowing through (forward outflow). Since the increase in pressure fluctuations begins at around 3.78 l/s, to study the onset of stall PIV images are recorded at and below 3.78 l/s, down to 2.52 l/s, at 0.12 l/s intervals. We record data when the stall related low-path-filtered, pressure signal is maximum, minimum and during zero crossing (growth of decay). We present results demonstrating the effects of: a. phase of the low path filtered pressure signal; b. blade orientation and c. flow rate.

Flow structures at different phases: Sample instantaneous vector maps at different phases of the stall, when the transducer signal at C is maximum, minimum and during zero crossing are presented in Figures 5a,b,c, respectively.

At minimum pressure, there is a reverse flow in the vane passage. The magnitudes of reverse velocities are only about 10% of the impeller tip speed. During zero crossing (Figure 5b) the lower vane passage is recovering from the reverse flow. At pressure maximum phase, there is a strong outward flow (Figure 5c). As the pressure in the vane passage rises it is able to overcome the high pressure in the volute just outside the diffuser; thereby resulting in outward flow. This process occurs at a characteristic frequency of 0.93 Hz.

Effect of blade orientation: Figure 6a,b,c and Figure 7a,b,c show phase averaged data (averages of 10 images, each) for the minimum and maximum pressure phases, at 3 different phase impeller orientations (–4°, 26°, 56°), respectively.

At the minimum pressure-phase, the phase-averaged data shows a reverse flow into passage C and a small positive flow in passage D. As the flow turns around back into the passage C
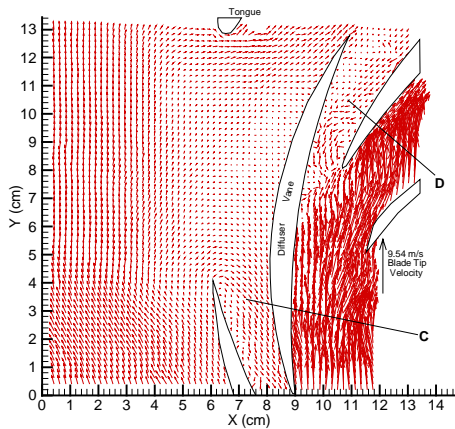
Copyright © 2000 by ASME

Figure 5(a): Instantaneous velocity map at minimum of the pressure signal from sensor C
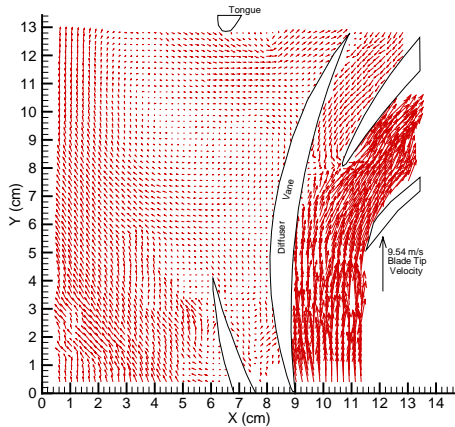

Figure 5(b): Instantaneous velocity map at zero-crossing (on the rise) of the pressure signal from sensor C
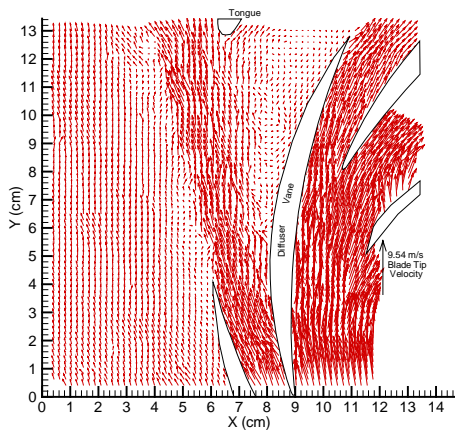

Figure 5(c): Instantaneous velocity map at a maximum point of the pressure signal from sensor C

it separates near the trailing edge of the lower diffuser vane. This separation results in a pocket of no flow or a vortex at the trailing edge, on the concave side of the lower vane. Also, several vortex structures/large eddies are seen in the volute, outside of the diffuser and near the exit (between the diffuser and tongue). Between instantaneous realizations these eddies vary both in strength and spatial locations.

At maximum pressure phase, there is an outward jet with velocity magnitude of about is 60% of the typical values on design condition. The separation point near the mid-chord region on the convex side of the central diffuser vane seems to shift around as the impeller blade passes by, but these fluctuations are small (Figure 7a,b,c). The leakage flow in the gap between the impeller and diffuser does not vary substantially with blade orientation. For both pressure minimum and pressure maximum, there is reverse flow into the impeller. However in pressure maximum phase, the leakage flow and reverse flow are much weaker. There is very little difference in the magnitude of the leakage flow except for the cases when the blade is located near the diffuser vane (Figure 7a), where the leakage decreases slightly.

In summary, it is shown that the flow patterns under stalled conditions have minimal dependence on the impeller orientation.

Effect of flow rate: Figures 8a,b to 11a,b present instantaneous and phase averaged velocity map at 3.78 l/s, 3.28 l/s, 3.02 l/s and 2.52 l/s, respectively for the cases of minimum pressure phase.

Typical narrow jetting near the concave side of the vane, with a wide separated region in the convex side, dominate the flow in and downstream of the diffuser at 3.78 l/s (Figure 8a, b). The flow near the concave surface contains several clockwise vortex structures. This same trend is also evident in the jet exiting from the previous diffuser passage (passage B), 40^0 upstream. This distribution is similar to that shown by Johnston and Dean (1966) during operation off-design flow rates. At 3.78 l/s, the jet always exists. With decreasing flow rate, from 3.78 to 3.53 l/s, the jet becomes weaker and the magnitude of the leakage velocity increases. The jet is intermittently replaced by a reversed flow, as demonstrated by the sample in Figure 9a. The frequency at which reversed flow is observed, increases with decreasing flow rate.

Below 3.28 l/s, the stalled area starts occupying two diffuser vane passages. The reverse flow magnitude also continues to increase as seen in Figure 10a, b. The jetting from passage B is still evident in the samples shown in Figure 9a and 10a, but dissapears on the phase averaged distributions in Figures 9b and 10b.

The 3.02 l/s level can be considered as the condition for which reverse flow regularly occurs at the pressure minimum phase. The sample of instantaneous flow already has two stalled vane passages (Figure 10a), but in the phase averaged data only channel C is stalled. At 2.52 l/s (Figure 11a,b), the flow is
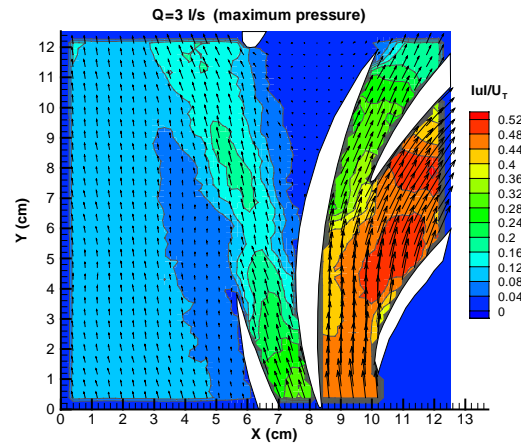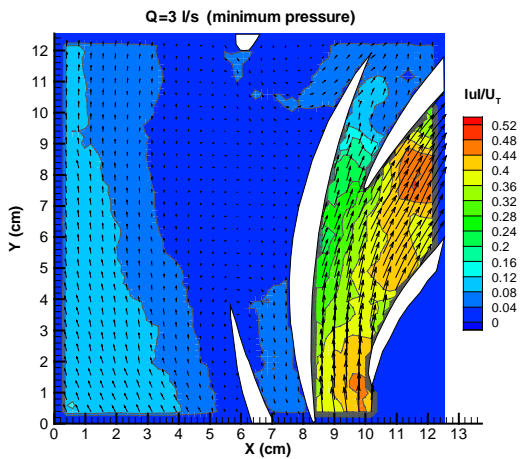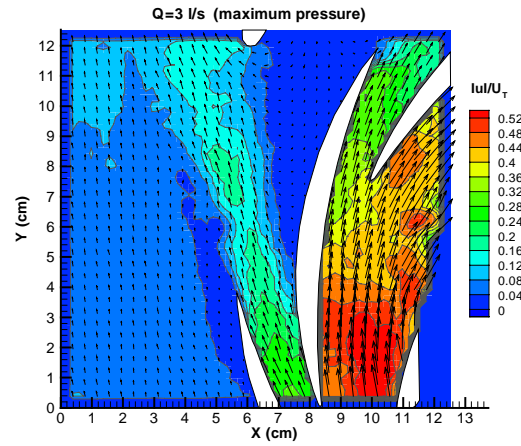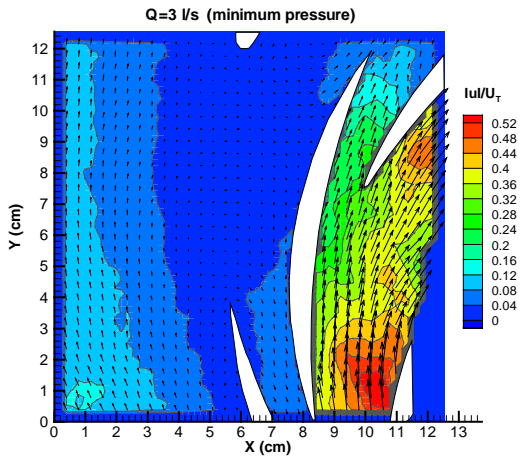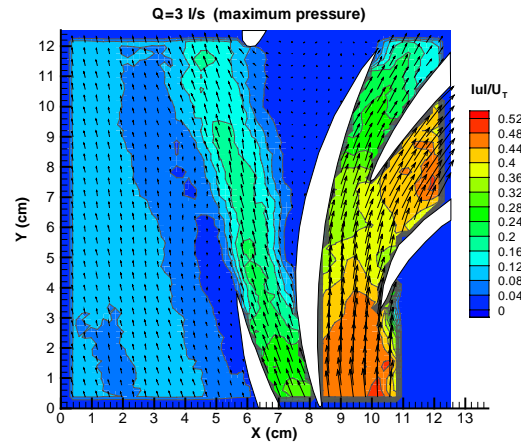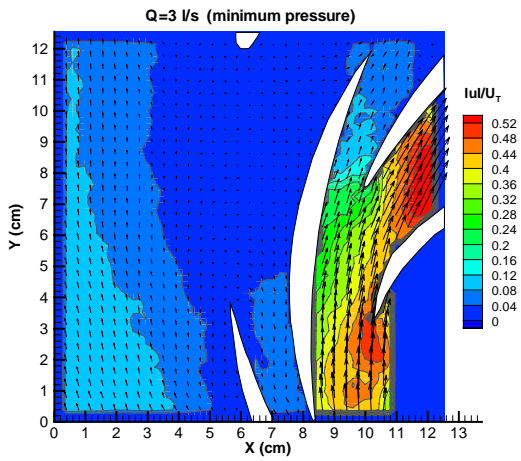
Figure 6a,b,c: Phase averaged velocity map in minimum pressure phase at −4, 26 and 56° blade orientation respectively (For reference length of vectors, see Figure 5)

Figure 7a,b,c: Phase averaged velocity map in maximum pressure phase at −4, 26 and 56° blade orientation respectively (For reference length of vectors, see Figure 5)
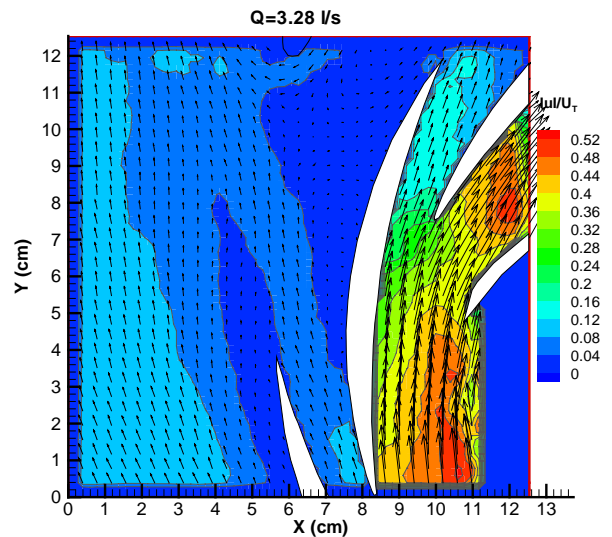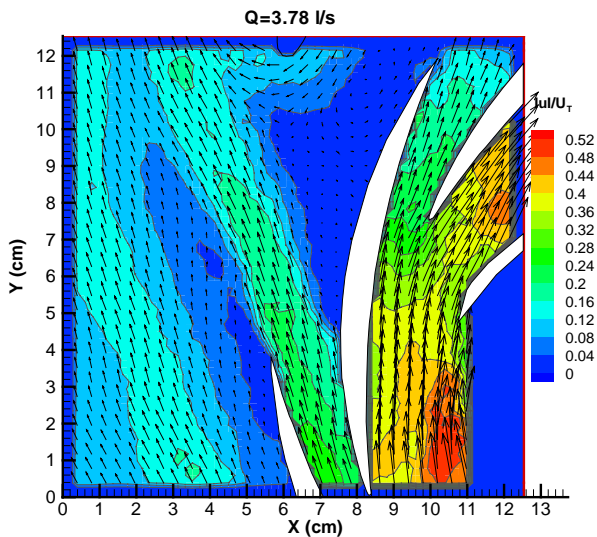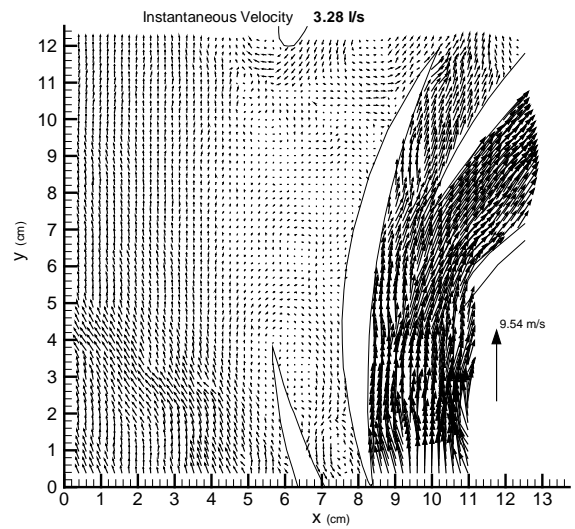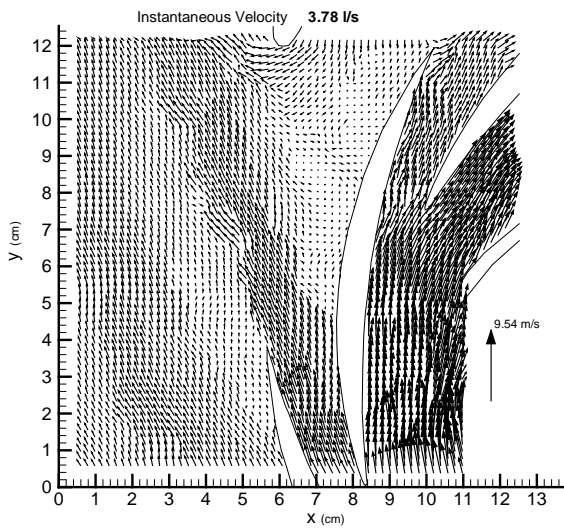
Figure 8a,b: Instantaneous and phase averaged velocity map in minimum pressure phase at 3.78 l/s flow rate level

Figure 9a,b: Instantaneous and phase averaged velocity map in minimum pressure phase at 3.28 l/s flow rate level

consistently reversed in both passages C and D during minimum pressure phase. Note that the reverse extends into the impeller, i.e. during stall there is backward flow into the impeller.

There are other interesting phenomena, for example, the magnitude of the leakage flow increases with decreasing flow rate, from about $0.42U_T$ at 3.78 l/s to $0.52U_T$ at 2.52 l/s. In the volute, the velocity increases with increasing distance from the diffuser on the left side of the vector maps in Figures 9b,10b and 11b. Near the tongue, there is flow from the beginning side of the volute towards the exit side of the volute. The magnitude of this secondary flow decreases with flow rate. This flow indicates that circumferential pressure gradients in the volute

are in the opposite direction compared to the gap between the impeller and diffuser.

CONCLUSIONS

Systematic PIV measurements are used for studying the flow structure within a centrifugal pump with a vaned diffuser under stall conditions. Effect of stall phase, flow rate and blade orientations are examined. The stall propagation frequency is 0.93 Hz. When the low path filtered pressure signal is maximum, there is a characteristic outward jet in the diffuser passage and the leakage is relatively small. During a pressure minimum phase, there is a reverse flow in the passage and the
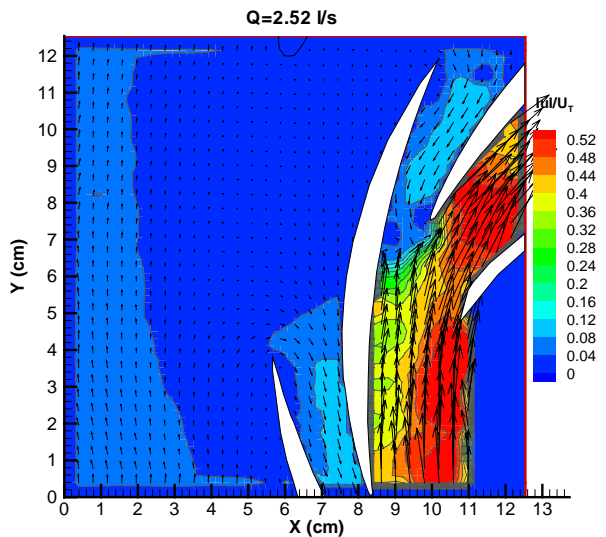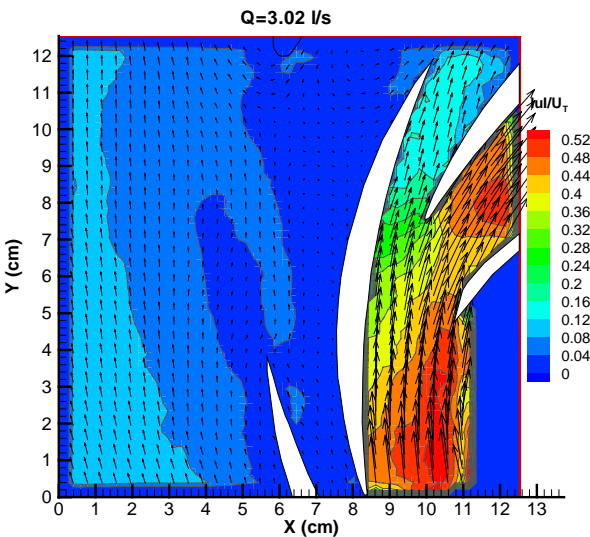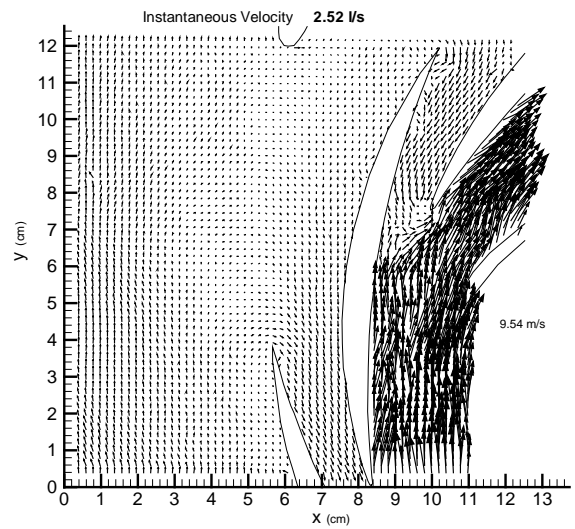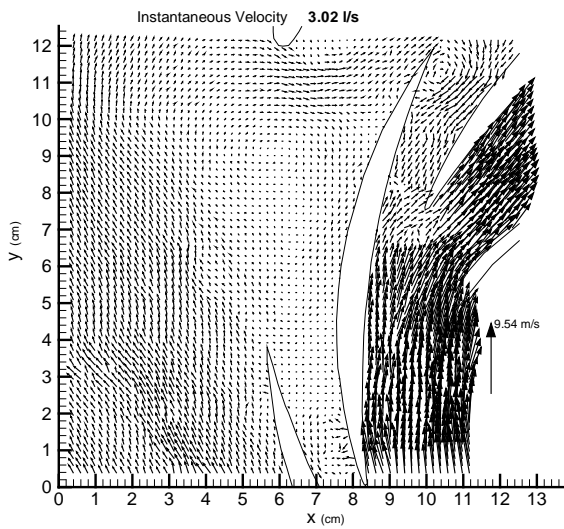
Figure 10a,b: Instantaneous and phase averaged velocity map in minimum pressure phase at 3.02 l/s flow rate level

Figure 11a,b: Instantaneous and phase averaged velocity map in minimum pressure phase at 2.52 l/s flow rate level

leakage increases substantially. There is also backward flow into the impeller. The blade orientation seems to have little impact on the flow within the diffuser except for the leakage. With decreasing flowrate, there is a substantial increase in magnitudes of reverse flow and leakage. The stall cell also increases in size.

ACKNOWLEDGMENTS

REFERENCES

Bertuccioli L, Gopalan S and Katz J, 1996, "Image Shifting for PIV using birefringent and ferroelectric liquid crystals", *Experiments in Fluids*, **21,** 341-346.

Braembussche VRA, 1996 "Flow and loss mechanisms in volutes of centrifugal compressor and pumps" *Von Karman Institute Lecture series,* 1996-01

Johnston J.P., and Dean R.C., 1966, "Losses in vaneless diffusers of centrifugal compressors and pumps" *ASME J. Eng. For Power*, **88,** 49-62

Longatte F., and Kueny JL, 1999 "Analysis of rotor stator circuit interactions in a centrifugal pump" FEDSM-**6866** *ASME Fluids Eng. Conf., San Francisco*

Miyake Y., Nagata T., 1999 "Full Simulation of a Flow in a Single Stage Axial-Rotor in Rotating Stall" FEDSM-**7197** *ASME Fluids Eng. Conf., San Francisco*

Ogata M and Ichiro A, 1995, "An experimental study of Rotating Stall in a Radial Vaned diffuser", *Unsteady Aerodynamics and Aeroelasticity of Turbomachines,* 625-641.

Roth G, Hart D and Katz J, 1995, "Feasibility of using the L64720 video motion estimation processor (MEP) to increase efficiency of velocity map generation for particle image velocimetry", *ASME/EALA Sixth Int. Conf. on Laser Anemometry,* Hilton Head, South Carolina.

Roth G and Katz J, 1999, "Parallel Truncated Multiplication and other methods for improving the speed and accuracy of PIV calculations", FEDSM-6998 *Proc. ASME Fluids Eng. Conf., San Francisco.*

Shuliang et al. 1999, "Three-Dimensional Turbulent Flow in a Centrifugal Pump Impeller Under Design and Off-Design operating Conditions" FEDSM-**6872** *Proceedings of the ASME Fluids Engineering Division* July 18-23, San Francisco

Sinha M and Katz J, 1998, "Flow Structure and Turbulence in a Centrifugal Pump with a vaned diffuser", FEDSM-**5129** *Proc. of the ASME Fluids Eng. Division,* Washington D.C.

Sinha M and Katz J, 1999, "The onset and development of rotating stall within a centrifugal pump with a vaned diffuser", FEDSM99-**7198** *Proc. of the ASME Fluids Eng. Division* July 18-23 San Francisco

Sinha M and Katz J, 2000a, "Quantitative Visualization of the flow in a centrifugal pump with diffuser vanes Part A: On flow structures and turbulence" *Jnl. Of Fluids En.g, in press*

Sinha M, Katz J, **Meneveau C.**, 2000b, "Quantitative Visualization of the flow in a centrifugal pump with diffuser vanes Part B: Addressing Passage Averaged and LES Modeling issues in turbomachinery flows" *Jnl. Of Fluids Eng., in press*

Tsujimoto Y., 1996 "Vaneless diffuser rotating stall and its control" *Von Karman Institute Lecture series,* 1996-01

Tsurusaki H., Kinoshita T., 1999 ,"Flow Control of Rotating Stall in a Radial Vaneless Diffuser" FEDSM99-**7199** *ASME Fluids Eng. Conf., San Francisco*

Yoshida Y, Murakami Y, Tsurusaki T, Tsujimoto Y, 1991, "Rotating Stalls in centrifugal impeller/vaned diffuser systems", *Proc. First ASME/JSME Joint Fluids Eng. Conf.,* **FED-107** , 125-130.